UDC 004.93

IMAGE SEGMENTATION WITH A CONVOLUTIONAL NEURAL NETWORK WITHOUT POOLING LAYERS IN DERMATOLOGICAL DISEASE DIAGNOSTICS SYSTEMS

Polyakova M. V. – Dr. Sc., Associate Professor, Professor of the Department of Applied Mathematics and Information Technologies, National University "Odessa Polytechnic", Odessa, Ukraine.

ABSTRACT

Context. The problem of automating of the segmentation of spectral-statistical texture images is considered. The object of research is image processing in dermatological disease diagnostic systems.

Objective. The aim of the research is to improve the segmentation performance of color images of psoriasis lesions by elaboration of a deep learning convolutional neural network without pooling layers.

Method. The convolutional neural network is proposed to process a three-channel psoriasis image with a specified size. The initial color images were scaled to the specified size and then inputed on the neural network. The architecture of the proposed neural network consists of four convolutional layers with batch normalization layers and ReLU activation function. Feature maps from the output of these layers were inputted to the 1×1 convolutional layer with the Softmax activation function. The resulting feature maps were inputted to the image pixel classification layer. When segmenting images, convolutional and pooling layers extract the features of image fragments, and fully connected layers classify the resulting feature vectors, forming a partition of the image into homogeneous segments. The segmentation features are evaluated as a result of network training using ground-truth images which segmented by an expert. Such features are robust to noise and distortion in images. The combination of segmentation results at different scales is determined by the network architecture. Pooling layers were not included in the architecture of the proposed convolutional neural network since they reduce the size of feature maps compared to the size of the original image and can decrease the segmentation performance of small psoriasis lesions and psoriasis lesions of complex shape.

Results. The proposed convolutional neural network has been implemented in software and researched for solving the problem of psoriasis images segmentation.

Conclusions. The use of the proposed convolutional neural network made it possible to enhance the segmentation performance of plaque and guttate psoriasis images, especially at the edges of the lesions. Prospects for further research are to study the performance of the proposed CNN then abrupt changes in color and illumination, blurring, as well as the complex background areas are present on dermatological images, for example, containing clothes or fragments of the interior. It is advisable to use the proposed CNN in other problems of color image processing to segment statistical or spectral-statistical texture regions on a uniform or textured background.

KEYWORDS: psoriasis image, image segmentation, convolutional network, pooling layer, color space, deep learning.

ABBREVIATIONS

BSA is the Body Surface Area;
PASI is the Psoriasis Area and Severity Index;
CNN is a convolutional neural network;
ReLU is a rectified linear unit;
TP is a number of true positive samples in percent;
TN is a number of true negative samples in percent;
FP is a number of false positive samples in percent;
FN is a number of false negative samples in percent;
FOM is a Figure of Merit.

NOMENCLATURE

I_I is the number of pixels of the psoriasis lesion edges, obtained by the proposed CNN;

I_A is the number of pixels of the psoriasis lesion edges on the ground-truth image;

α is a scale factor;

d_i is the distance between the pixel of the psoriasis lesion edge, obtained by the proposed CNN, and the pixel of the psoriasis lesion edge on the ground-thruth image, measured along the normal to this edge.

INTRODUCTION

Medical diagnostic systems are widely used in the field of health care. In particular, such systems can provide information about the pathologies based on medical images. For example, various datasets related to the treatment of dermatological diseases have been collected. A number of datasets include images obtained during the diagnosis of psoriasis. The World Health Organization statistics estimate the number of patients suffering from this disease at 125 million people. According to the International Federation of Psoriasis Associations, the prevalence of this disease depends on the region and ranges from 1.2% to 5%, averaging 3% of the general population [1].

The disease of psoriasis is accompanied by unpleasant sensations such as peeling and itching of the affected areas of the skin, causing discomfort to the patient, and is also a systemic disease, often accompanied by arthritis, diabetes, cardiovascular diseases, etc. To diagnose and monitor the effectiveness of treatment, psoriasis lesions are isolated on photographs of the patient's skin and evaluate their geometric characteristics. The values of these characteristics are used in assessing the clinical severity of psoriasis using the BSA and the PASI [2].

DOI 10.15588/1607-3274-2023-1-5

The identification of psoriasis lesions on skin images by a dermatologist requires a significant time and effort. In addition, since there are other skin diseases similar to psoriasis, then the diagnosis of psoriasis also requires significant experience of a specialist in the field of dermatology. Therefore, medical diagnostic systems are used to perform automated processing of images of psoriasis lesions [3–5].

The object of research is image processing in dermatological disease diagnostic systems.

To assess the clinical severity of psoriasis using the BSA and PASI indexes in dermatological disease diagnostic systems, the results of segmentation of skin images are needed to identify the psoriasis areas [4]. Segmentation of color images of skin affected by psoriasis is a difficult problem due to uneven or insufficient lighting, irregular shape and different sizes of psoriasis lesions, blurred boundaries between lesions and normal skin. In addition, the result of segmentation of images of psoriasis lesions is affected by skin pigmentation and texture that varies from person to person, the presence of hair, as well as the type of skin (dry, oily or combination), which determines its reflectivity.

The subject of the research is the methods of segmentation of color images of psoriasis lesions.

Methods for segmenting color images of psoriasis lesions that do not use convolutional neural networks (CNNs) are generally characterized by low performance [6–8], which is due to the natural variability of human skin and the size of psoriasis lesions. So, plaque psoriasis is often characterized by the lesions of considerable size, while guttate psoriasis is appeared by small lesions. The psoriasis image segmentation is also significantly affected by the experience of the researcher and the segmentation feature selection. Therefore, deep learning CNNs have recently been used to segment color images of psoriasis lesions, providing automatic feature selection [9–10]. The most common architecture of such networks includes convolutional layers, pooling layers and fully connected layers. When segmenting images, convolutional and pooling layers extract the features of image fragments, and fully connected layers classify the resulting feature vectors, forming a partition of the image into homogeneous segments. The pooling layers of the CNN are reduce the size of image feature maps, but negatively affects on the segmentation performance, especially for the images of the small psoriasis lesions and complex-shaped psoriasis lesions.

The aim of the research is to improve the of segmentation performance of color images of psoriasis lesions by elaboration of a deep learning CNN without pooling layers.

1 PROBLEM STATEMENT

The color image of psoriasis lesions is represented by the vector function $\mathbf{I}(x,y)=(I_R(x,y), I_G(x,y), I_B(x,y)\}$, where $x=1, \ldots, n$; $y=1, \ldots, m$; n, m are positive integers, n is the number of rows, m is the number of columns of the image. The intensities of the color components $I_R(x,y)$, $I_G(x,y)$, $I_B(x,y)$ take values from the interval [0, 1]. Then each pixel of the image with coordinates (x,y) is described by three features, namely intensities of color components with values $I_R(x,y)$, $I_G(x,y)$, $I_B(x,y)$. To identify the psoriasis lesions on the image, it is necessary to segment it into non-overlapping regions corresponding to regions of lesions and normal skin. To do this, each pixel of the original image must be associated with the value of the target feature. There is a label of one of two classes, specifically, 0 for normal skin, 1 for psoriasis lesion. The values of the target feature for the psoriasis image should be represented as a binary image which is the result of segmentation.

To segment the color images of psoriasis lesions, a CNN elaboration is needed. The CNN input is a three-dimensional matrix of intensity values of color components for image pixels. At the output of this network, a two-dimensional matrix of target feature values is obtained for each image pixel. To construct a convolutional neural network $CNN = \{struct, param\}$, it is necessary to select its architecture *struct* and evaluate network parameters *param* so as to minimize the cost function on the training set [11, 12]. It is assumed that the training set includes psoriasis images and corresponding ground-truth images for CNN parameters learning.

2 REVIEW OF THE LITERATURE

An analysis of the literature shows that psoriasis image processing implies either classification of such images to determine the severity of the disease [13–15] or psoriasis image segmentation [16–18], since the area of psoriatic lesions is taken into account when determining the severity of the disease and evaluating the effectiveness of treatment [2, 4, 10]. When selecting and evaluating the psoriasis image features it is important to consider that normal skin regions differ from psoriasis lesions both in color and texture. For example these regions can be distinguished by the values of the amplitude and frequency of the components of the spectral texture [19, 20]. Therefore, single-scale and multi-scale methods are presented in the literature for psoriasis image processing.

Single-scale methods use color features and/or spectral features at the dominant frequency. Such methods segmenting psoriasis image into areas of normal skin and psoriasis lesions, based on the feature vectors calculated in the neighborhood of each pixel. The the resulting segmentation performance depends on the parameter values setting. In addition there are difficulties in segmenting objects of different sizes and setting of parameters.

Thus, in [7], two color spaces were used to segment psoriatic plaques on skin images, namely CIE Luv and CIE Lch. In the CIE Luv space, the color feature vectors of the pixels were clustered based on the Gaussian mixture model, and in the CIE Lch color space, a semi-wrapped Gaussian mixture model was proposed to solve this problem. For the localization of plaques on the skin, the von Mises distribution was assumed to determine the

DOI 10.15588/1607-3274-2023-1-5

confidence intervals for the distribution parameters of normal skin and plaque color. This approach showed a higher segmentation performance compared to the fuzzy c-means, the segmentation accuracy was 79.53%.

In [8], a method for texture segmentation of plaque psoriasis images was elaborated for express diagnostic systems in dermatology. Psoriasis lesions on the images were modelled as fragments of a quasi-periodic texture on a complex background with additive Gaussian noise. To segmenting psoriasis lesions, there was used sequentially the localization of spatial frequencies of the image; the amplitude detecting that transforms the texture features into intensity; the edge detection of the resulting image. Then 87% of image pixels were correctly segmented by this method.

In [6], for the segmentation of color psoriasis images the RGB images convert to the Lab space, and then k-means clustering was applied to the color feature vectors of image pixels. To improve the segmentation performance the merged group of pixels was filtered, as a result of which correctly segmented pixels averaged 95%.

In [19, 20], for systems of express diagnostics of psoriasis, skin images were represented by a spectral-statistical texture. The vector-difference method was applied for image segmentation. This method is based on the calculation of distances between feature vectors of image pixel neighborhoods. Each feature vector is involved the mean value and the standard deviation of the intensities of the neighborhood pixels. For images of plaque psoriasis, the percentage of correct pixel segmentation was 92.7%, and for pixels of lesions of plaque psoriasis, up to 96%, depending on the signal-to-noise ratio.

Multiscale methods are elaborated for segmenting the lesions of different sizes on psoriasis images. However, there are difficulties when combining the results of segmentation at different scales. For example, in [21], a method for segmenting ot the psoriasis images in the Lab color space was proposed. In this space, multi-scale superpixels of images were identified, and superpixels that did not correspond to the skin areas were discarded. Next, at each scale, the superpixels were k-means clustered. The merging of segmentation results at different scales was performed using voting. Correctly segmented pixels in the images were about 90%. The method has shown its effectiveness in the treatment of skin with hair, and with lesions of different sizes and shapes.

A separate group of multiscale methods are CNNs that are used both for segmentation and for classifying of psoriasis images.

In [3], a classification system for skin diseases was developed, implemented as Android application based on the MobilNet. This network alternates convolutional layers and depthwise separable convolutions with depthwise and pointwise layers. Each of these 27 layers was followed by batch normalization and a ReLU activation function. The average percentage of correct recognition of the seven skin diseases reached 94.4% after oversampling to balance the data set and pre-process the researched images.

In [13], images of psoriasis lesions were classified into images of plaque psoriasis and guttate psoriasis. A CNN was used with two convolutional layers, followed by pooling layers, then two fully connected layers were applied. Correct image recognition of plaque and guttate psoriasis was 82.9% and 72.4%.

In [4], psoriasis images were analyzed to automaticall form the severity of the disease. The severity of the psoriasis are assessed on the basis of the erythema or redness level, the degree of scaliness, the thickness or induration of psoriasis plaques on the human skin. The percentage of the body surface area affected by psoriasis also included in PASI estimation. Psoriasis images were classified by a CNN that consisted of a shared subnet followed by three parallel subnets. At the output of these subnets, the level of the disease severity was obtained for each of the three features as an integer from 0 to 4. The shared subnet consisted of 5 convolutional layers with the ReLU activation function and normalization after the 1st and 2nd layers, as well as three pooling layers after the 1st, 2nd, 5th convolutional layers. Subnets for each feature included 2 fully connected layers with the ReLU activation function, after which the SoftMax activation function was applied. The correct recognition of the severity scores based on the each feature was 60%, and about 94% if assuming a maximum deviation ±1 from the actual scores for any of erythema, scaling and induration scores. Under this assumption, the correct recognition of the severity scores is 85.3%.

In [9], a modified U-Net architecture referred as PsLSNet was proposed for the segmentation of psoriasis images. It is a deep learning CNN with 29 layers. By reducing the covariant shift through the implementation of PsLSNet, the training time is reduced compared to U-Net. The PsLSNet network is able to segment psoriasis images even under poor acquisition conditions and in the presence of artifacts. The average percentage of correctly segmented pixels was 94.8% with a sensitivity of 89.6% and a specificity of 97.6%.

In [10], it was assumed that psoriasis images may be blurred or contain areas of a complex background. For the segmentation of such images, a YOLACT CNN has been developed, which includes four consecutive subnets. These are a subnet for evaluating segmentation features, a subnet for generating feature maps at different image scales, a subnet for classifying the obtained feature vectors, and a subnet for generating the result of segmentation and post-processing. Correct segmentation of image pixels was achieved in 96–97% of cases.

The analysis of methods of psoriasis image segmentation showed that the main characteristic of these methods is the segmentation performance, which is affected by the shape and sizes of isolated lesions that differ for plaque and guttate psoriasis. In the case of express diagnostics, the time of image processing is also significant.

DOI 10.15588/1607-3274-2023-1-5

Single-scale methods are characterized by high speed, but the segmentation performance is low, especially when identifying small psoriasis lesions and complex-shaped psoriasis lesions. The results of image segmentation often contain defects in the form of small regions at the boundaries of areas corresponding to psoriasis lesions. In addition, parameters setting are time consuming for single-scale methods.

Multiscale methods are characterized by a higher performance of psoriasis image segmentation due to the better localization of the boundaries of psoriasis lesions. However, these methods are often unable to segment the small lesions or fragments of lesions of complex shape, mistaking them for areas of healthy skin. If the multiscale methods of psoriasis image segmentation don't use the CNN, then it is necessary for the researcher to select segmentation features, the procedure for their evaluation, and a method for combining segmentation results at different scales. The use of CNN allows to avoid these difficulties, since segmentation features are evaluated as a result of network training using ground-truth images which segmented by an expert. Such features are robust to noise and distortion in images. The combination of segmentation results at different scales is determined by the network architecture. However, deep learning CNN contains a large number of layers and, accordingly, is characterized by a significant number of parameters. The training of such CNN requires a large training set, and the complexity of the architecture increases the network training time. In addition, a common drawback of the CNN in solving the problem of psoriasis image segmentation is the low performance if objects of small sizes or complex shapes are processed. This due to the inclusion of pooling layers in the network architecture, which reduce the scale of image feature maps.

3 MATERIALS AND METHODS

The proposed neural network is elaborated to process a three-channel image with a size of 224×224 pixels. Therefore, the initial color images were scaled to the specified size and then giving them as input of the neural network. The architecture of the proposed neural network is shown in Table 1. This CNN contains five convolutional layers, four batch normalization layers, four ReLU activation function layers, one Softmax activation function layer, and one image pixel classification layer. The first convolutional layer uses 18 convolution kernels of size 85×85×3 pixels with a stride of 1 pixel. The feature maps at the output of this layer are batch normalized and then the ReLU activation function is applied. Next, feature maps from the output of the ReLU activation function layer, were inputed to the second convolutional layer, which uses 18 convolution kernels of size 55×55×3 pixels with a stride of 1 pixel. The feature maps at the output of this layer are also batch normalized and then the ReLU activation function is applied again. The resulting feature maps were inputed to the third convolutional layer, which uses 18 convolution kernels of size 35×35×3 pixels with a stride of 1 pixel. The feature maps at the output of this layer are again batch normalized, and then the ReLU activation function is applied again. It is followed by the fourth convolutional layer, which uses 18 convolution kernels of size 15×15×3 pixels with a stride of 1 pixel. The obtained feature maps at the output of this layer are batch normalized, and then the ReLU activation function is applied again. Feature

Table 1 – The proposed CNN architecture

Layer number	Type	Comment	Activations	Learnables
1	Image Input	256×256×3 images with zero center normalization	224×224×3	–
2	Convolution	18 85×85×3 convolutions with stride [1 1] and same padding	224×224×18	Weights: 85×85×3×18 Bias: 1×1×18
3	Batch normalization	Batch normalization with 18 channels	224×224×18	Offset: 1×1×18 Scale: 1×1×18
4	ReLU	Activation function	224×224×18	–
5	Convolution	18 55×55×3 convolutions with stride [1 1] and same padding	224×224×18	Weights: 55×55×3×18 Bias: 1×1×18
6	Batch normalization	Batch normalization with 18 channels	224×224×18	Offset: 1×1×18 Scale: 1×1×18
7	ReLU	Activation function	224×224×18	–
8	Convolution	18 35×35×3 convolutions with stride [1 1] and same padding	224×224×18	Weights: 35×35×3×18 Bias: 1×1×18
9	Batch normalization	Batch normalization with 18 channels	224×224×18	Offset: 1×1×18 Scale: 1×1×18
10	ReLU	Activation function	224×224×18	–
11	Convolution	18 15×15×3 convolutions with stride [1 1] and same padding	224×224×18	Weights: 15×15×3×18 Bias: 1×1×18
12	Batch normalization	Batch normalization with 18 channels	224×224×18	Offset: 1×1×18 Scale: 1×1×18
13	ReLU	Activation function	224×224×18	–
14	Convolution	2 1×1×18 convolutions with stride [1 1] and same padding	224×224×2	Weights: 1×1×18×2 Bias: 1×1×2
15	Softmax	Activation function	224×224×2	–
16	Pixel classification	–	–	–

DOI 10.15588/1607-3274-2023-1-5

maps from the output of this layer were inputted to the fifth convolutional layer, which uses 2 convolution kernels of size 1×1×18 pixels with a stride of 1 pixel, then the Softmax activation function is applied. The resulting feature maps were applied to the image pixel classification layer.

In the convolution layer, the matrix of the convolution kernel moves through a two-dimensional array of image pixels. The values of the corresponding image elements and the convolution kernel are multiplied the results are added up and inputted on the next layer. Usually, several convolution kernels are used in the convolution layer. In addition, it is the stride parameter, which indicates the convolution kernel shift along the image matrix.

Batch normalization layer solves vanishing gradient problem and train deep neural networks consisting of a few dozen layers. It is known that the error backpropagation algorithm converges faster if the input data is normalized (has zero mean and unit variance) [13]. However, when a signal propagates through a neural network, its mean value and variance can change significantly. To avoid this, the standard normalization of the outputs of the convolutional layer is performed by subtracting from each output x_i the average value μ_i of the input packet examples by dimension i and dividing by $(\sigma_i+\varepsilon)^{0.5}$, where σ_i is the standard deviation of the input packet images by dimension i, ε is a constant that ensures the stability of calculations. However, normalizing the output of a neural network convolutional layer can change the representation of the data in the next layer. Therefore, two parameters are introduced: compression γ_i and shift β_i of the normalized value for each output, which are adjusted in the learning process along with the rest of the parameters and transform the normalized output value x_{ni} as $y_i=\gamma_i x_{ni}+\beta_i$. For convolutional neural networks, batch normalization reduces training time and reduces the chance of overfitting.

The ReLU activation function ReLU(y)=max(0,y) returns 0 for a negative argument, and in the case of a positive argument, returns the same. The advantages of this function over the sigmoid are the fast calculation of the derivative (for negative arguments it is 0, for positive ones it is 1), and the sparseness of activation (fewer neurons being activated).

Pooling layers were not included in the architecture of the proposed CNN since they reduce the size of feature maps compared to the size of the original image and can decrease the segmentation performance of small psoriasis lesions and psoriasis lesions of complex shape.

4 EXPERIMENTS

As a result of the experiment, the segmentation performance was estimated for 50 images of psoriasis lesions from the [22]. The researched images contained only areas of healthy skin and psoriasis lesions. Areas corresponding to the background were absent. The image sizes varied as follows. For the images of plaque psoriasis the height varied from 200 to 380 pixels, and the width varied from 180 to 500 pixels. The height of the images of guttate psoriasis varied from 400 to 800 pixels, the width from 300 to 530 pixels. These images were marked by an expert on areas of normal skin and psoriasis lesions. Then the segmentation performance was estimated by confusion matrices [23, 24]. Since psoriasis images were segmented on health skin and psoriasis lesions, then the confusion matrix of size 2×2 consists of the following elements. TP is the percentage of image pixels from the class labeled “Normal skin” that are correctly assigned to the class labeled “Normal skin”; FP is the percentage of image pixels from the class labeled “Psoriasis lesion” that are incorrectly assigned to the class labeled “Normal skin”; FN is the percentage of image pixels from the class labeled “Normal skin” incorrectly assigned to the class labeled “Psoriasis lesion”; TN is the percentage of image pixels from the class labeled “Psoriasis lesion” that are correctly assigned to the class labeled “Psoriasis lesion”.

To characterize the detection of the edges of psoriasis lesions, the FOM value [25] was used:

$$FOM = \frac{1}{I}\sum_{i=1}^{I_A}\frac{1}{1+\alpha d_i^2}.$$

where I=max(I_I, I_A). The FOM value is normalized such that FOM=1 for a well detected edge. The factor 1/I characterizes doubled and split edges.

When training the proposed CNN, a cross-entropy loss function was used, for which the relative frequencies w and 1–w of the appearance of pixels of the “Normal skin” and “Psoriasis lesion” classes were taken into account. For each image pixel, the value of cross-entropy L was calculated by the formula

$$L = -(1/w)\, t_1 \log_2 y_1 - 1/(1-w)\, t_2 \log_2 y_2,$$

where t_i = 1 if the image pixel is assigned to class i on the ground-thruth image, otherwise t_i = 0, with i = 1 for the class “Normal skin” and i = 2 for the class “Psoriasis lesion”. The y_i value is the result of calculating the value of the Softmax function for the image pixel under consideration. It is interpreted as the probability that an image pixel belongs to the class “Normal skin” (i = 1) or “Psoriasis lesion” (i = 2). To calculate the cross-entropy of the image, the values of L were summed over all its pixels.

First, as part of the experiment, RGB, Lab, YCbCr, HSV, YIQ, XYZ color spaces were used to represent images of psoriasis lesions [26]. In this part of experiment the proposed CNN and U-Net [27] consisting of four levels reliazed by 3×3 convolutions are researched. The stochastic gradient descent with a moment of 0.9 and an initial learning rate of 0.01 was used to train the proposed CNN. The Adam method with an initial learning rate of 0.0001 was used to train the U-Net.

Note that the color images of lesions of plaque and guttate psoriasis differ significantly in their properties, primarily in the size of the lesions, as well as their color

DOI 10.15588/1607-3274-2023-1-5

and texture. Plaque psoriasis usually presents by red or light gray lesions of considerable size with coarse grained texture, while guttate psoriasis presents by small reddish lesions of fine texture. Therefore, in this research, segmentation performance was evaluated separately for images of plaque and guttate psoriasis, in contrast to the papers [6–10, 19–21] and others, in which segmentation performance measures were averaged over images of both classes.

Second, as part of the experiment, the Adam method with an initial learning rate of 0.05 and the stochastic gradient descent with a moment of 0.9, and an initial learning rate of 0.01 was used to train the proposed CNN on the researched psoriasis images. To avoid overfitting of the network, training was stopped when the value of the loss function began to increase. The number of training epochs depended on the color space in which the images were presented.

Third, as part of the experiment, the psoriasis image segmentation performance for the proposed CNN was compared with the known segmentation methods [6–10, 19–21]. The accuracy measure is used. It represents the integral characteristic of the segmentation performance calculated by averaging of *TP* and *TN*.

And at last, the comparison of processing time was made for the image segmentation by the proposed CNN and the U-Net [27] for the researched psoriasis images scaled to a size of 224×224 pixels.

5 RESULTS

The elements of confusion matrices for the results of psoriasis image segmentation with representation in different color spaces is shown in Table 2. Values in this table were obtained by averaging the *FOM*, *TP*, and *TN* for the segmentation of plaque psoriasis images, guttate psoriasis images, and all the researched psoriasis images.

Table 2 – The values of TP and TN for the results of segmentation by the proposed CNN and U-Net of psoriasis images represented in different color spaces

Color space	Plaque psoriasis images			Guttate psoriasis images			All researched psoriasis images		
	TR	*TN*	*FOM*	*TR*	*TN*	*FOM*	*TR*	*TN*	*FOM*
Proposed CNN									
RGB	98.48	99.55	0.7844	93.41	91.83	0.7637	95.53	96.78	0.7741
Lab	98.37	99.72	0.7256	91.57	88.01	0.5102	94.42	95.51	0.6179
HSV	97.92	99.56	0.7671	89.75	87.05	0.5996	93.17	95.07	0.6834
YIQ	97.51	99.40	0.7917	93.60	87.98	0.6591	95.24	95.30	0.7254
YCbCr	97.72	99.73	0.6568	93.29	87.33	0.5240	95.14	95.28	0.5904
XYZ	96.04	98.42	0.5854	91.34	80.94	0.5597	93.31	92.15	0.5730
U-Net									
RGB	95.78	99.46	0.4034	88.89	91.70	0.3995	91.77	96.67	0.4014
Lab	95.29	98.77	0.4413	88.91	87.93	0.4524	91.58	94.88	0.4469
HSV	98.00	99.66	0.3689	82.27	90.89	0.3573	86.34	96.51	0.3631
YIQ	94.76	99.67	0.4196	83.52	95.02	0.3821	88.22	98.00	0.4009
YCbCr	96.14	99.61	0.5461	87.91	94.00	0.5167	91.35	97.60	0.5314
XYZ	94.29	97.88	0.3372	87.53	86.21	0.3945	90.36	93.69	0.3658

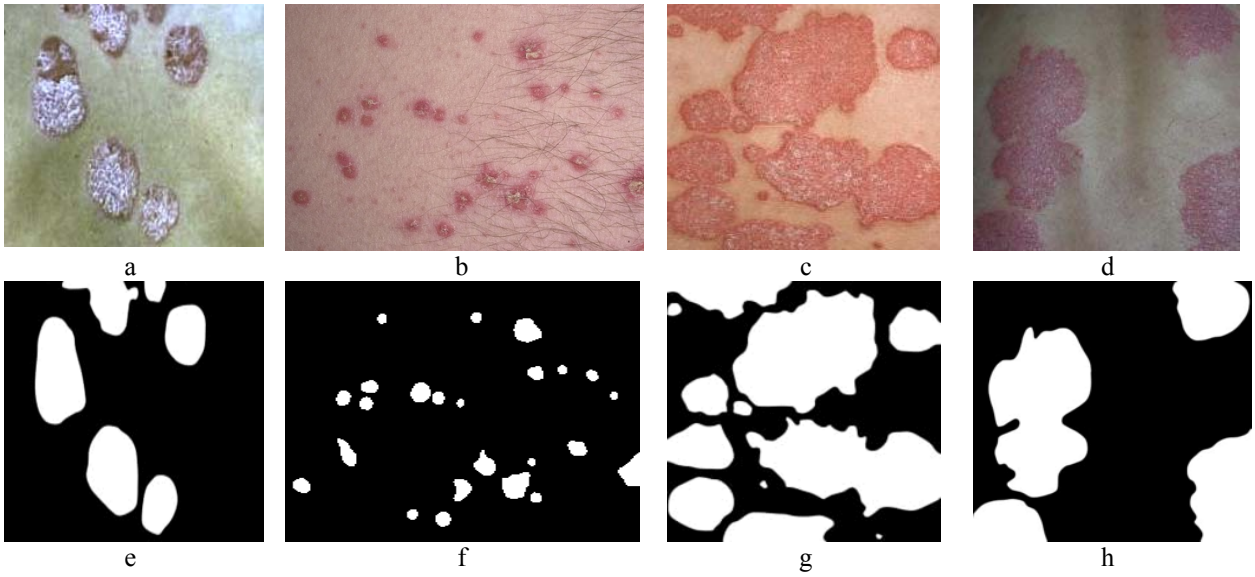

a b c d

e f g h

DOI 10.15588/1607-3274-2023-1-5

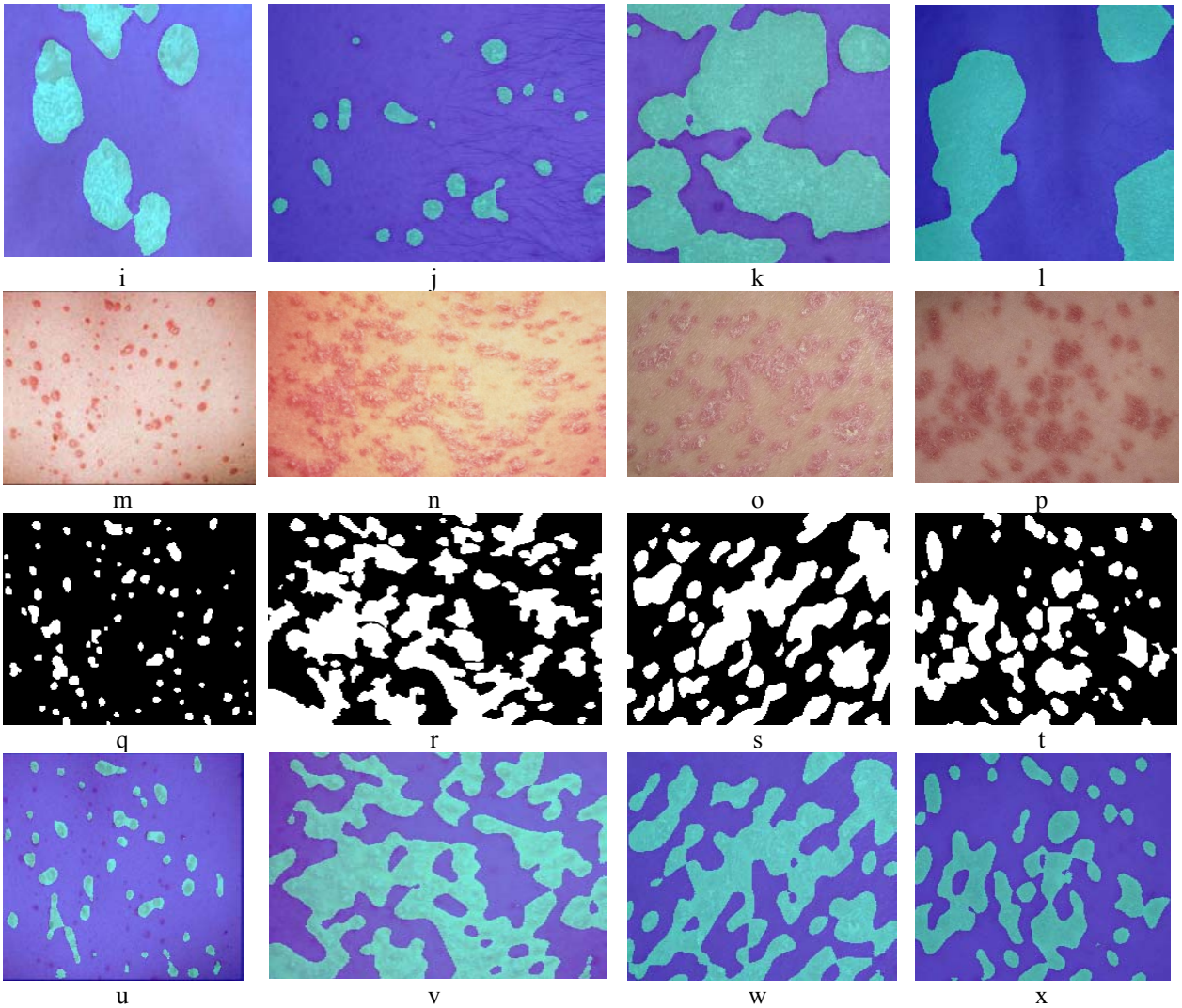

Figure 1 – The segmentation results by proposed CNN:
a–d, m–p – the initial psoriasis images; e–h, q–t – the ground-truth images; i–l, u–x – images, segmented by proposed CNN

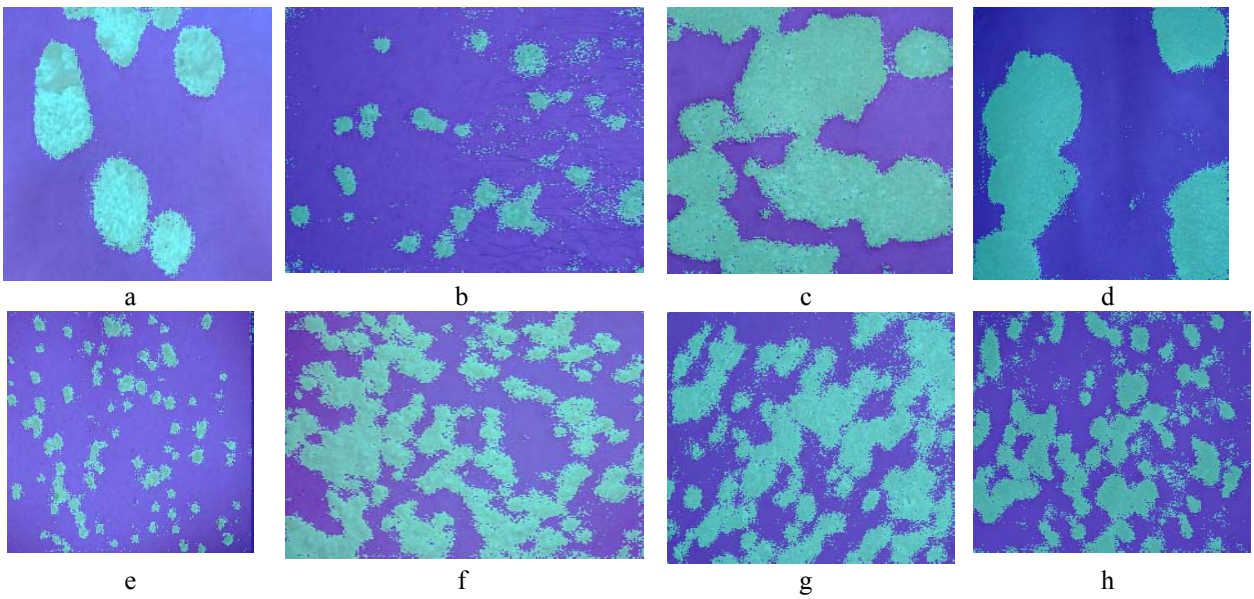

Figure 2 – The segmentation results by U-Net:
a–d – the psoriasis images from Figure 1, a–d, segmented by U-Net; e–h – the images from Figure 1, m–p, segmented by U-Net

DOI 10.15588/1607-3274-2023-1-5

The accuracy of the psoriasis image segmentation by the proposed CNN, the U-Net, and methods known from the literature are given in Table 3.

Table 3 – The segmentation accuracy of the proposed CNN and methods known from the literature

Reference, publication year, network name	Segmentation accuracy, %
Single Scale Methods	
[7], 2015	79.53%
[8], 2019	87.20%
[19], 2022	92.68%
[6], 2017	95%
Multiscale Methods	
[21], 2017	90%
[9], 2019, PsLSNet	94.8%
[10], 2021, YOLACT	96.6–97.3%
Proposed CNN, RGB images of plaque psoriasis	99.02%
Proposed CNN, RGB images of guttate psoriasis	92.62%
Proposed CNN, Lab images of plaque psoriasis	99.05%
Proposed CNN, Lab images of guttate psoriasis	89.79%
Proposed CNN, YIQ images of plaque psoriasis	98.46%
Proposed CNN, YIQ images of guttate psoriasis	90.79%
[27], 2015, U-Net, RGB images of plaque psoriasis	97.62%
[27], 2015, U-Net, RGB images of guttate psoriasis	90.30%
[27], 2015, U-Net, Lab images of plaque psoriasis	97.03%
[27], 2015, U-Net, Lab images of guttate psoriasis	88.42%
[27], 2015, U-Net, YIQ images of plaque psoriasis	97.22%
[27], 2015, U-Net, YIQ images of guttate psoriasis	89.27%

Fig. 1 illustrates the psoriasis images, the ground-truth images, and the segmentation results, obtained by proposed CNN. At Fig. 2 it is shown the segmentation results, obtained by U-Net which consist of four levels reliazed by 3×3 convolutions. It can be seen from the Fig. 1 that image segmentation by the proposed CNN is characterized by high accuracy in detection of the psoriasis lesion edges.

6 DISCUSSIONS

Analysis of the segmentation performance measures given in Table 2 showed the following. It is preferable to segment images of guttate psoriasis lesions in color spaces in which either the red component is isolated separately (RGB), or there is a difference component of red and another color (Lab, YCbCr, YIQ). This is due to the fact that the lesions of guttate psoriasis differ from normal skin mainly by redness level.

Thus, the highest performance of image segmentation of guttate psoriasis lesions by the proposed CNN was obtained using the RGB color space. The Lab, YIQ, YCbCr spaces showed similar results, but compared to the use of the RGB space, TP decreased to 2%, TN decreased by 4%. The presentation of images of guttate psoriasis lesions in xyz and HSV spaces showed the worst results compared to RGB. Specifically, TP is less by 2–4%, TN is less by 4–11%. For images of lesions of plaque psoriasis in the researched color spaces, the segmentation performance mainly differed within the statistical error. Further, for guttate psoriasis images more often image pixels from the class labeled “Psoriasis lesion” were incorrectly assigned to the class labeled “Normal skin”. For plaque psoriasis images, on the contrary, more often the pixels from the class labeled “Normal skin” were incorrectly assigned to the class labeled “Psoriasis lesion”. This result is due to the relative size of lesions of plaque and guttate psoriasis compared to the normal skin areas in the researched images. Plaque psoriasis lesions occupied a significant area on the researched images; guttate psoriasis lesions are much smaller in area.

The use of U-Net for psoriasis image segmentation [27] instead of the proposed CNN did not improve the segmentation performance.

The proposed CNN is shown a particulary significant advantage in detection of the psoriasis lesion edges. For U-Net the FOM values is less by 17–53% with median 40% for plaque psoriasis images, and the FOM values is less by 2–47% with median 40% for guttate psoriasis images, as compared with the proposed CNN. For all researched psoriasis images the FOM values of U-Net segmentation is less by 10–48% with median 40%.

Next, the Adam method is used for training the proposed CNN. In this case the lower segmentation performance is obtained as compared to stochastic gradient descent. For guttate psoriasis images, TP is less by 3–7%, and TN is decreased by 5–11%, for plaque psoriasis images TP is less by 3%.

Analysis of the segmentation performance of the proposed CNN and the known segmentation methods [6–10, 19–21] given in Table 3 showed the following. The percentage of correctly segmented pixels (accuracy, %) of the proposed CNN exceeds the known methods by up to 13% for guttate psoriasis images and by 4–20% for plaque psoriasis images.

A comparison of processing time was made for the image segmentation by the proposed CNN and the U-Net [27]. The researched psoriasis images were scaled to a size of 224×224 pixels. Then the processing time of the proposed CNN was 3.7–3.8 seconds on average per image when training the network using the stochastic gradient descent method. For a 4-level UNet network, when trained by the Adam method, the average processing time for one image with a 3 × 3 filter was 1.9–2 seconds. The research was performed using an Intel Core i5-7400 processor, 3 GHz CPU, 16GB memory, Windows 10 operating system, 64 bit. Thus, the proposed CNN requires on average 2 times more time to process one image than the 4-layer U-Net network. However, the number of training epochs of the 4-layer U-Net for this segmentation problem is, on average, 30–40% more than is required for training the proposed CNN.

CONCLUSIONS

The problem of mathematical support elaboration is solved to automate the image processing in dermatological disease diagnostic systems.

DOI 10.15588/1607-3274-2023-1-5

The scientific novelty of obtained results is that the deep learning convolutional neural network was elaborated to segment color psoriasis images. The improved CNN differs from those known from the literature in that its architecture did not include pooling layers; only convolutional layers, batch normalization, and an activation function were used. The use of the proposed CNN made it possible to enhance the segmentation performance of plaque psoriasis images and, especially, guttate psoriasis images at comparable processing time. There were no abrupt changes in color and illumination, blurring, as well as the complex background, for example, containing clothes or fragments of the interior on the researched psoriasis images. For such images, in cases of slow changes in image illumination, the proposed CNN showed a high segmentation performance, especially at the edges of the lesions.

The practical significance of obtained results is that the software realizing the proposed CNN is developed, as well as experiments to research its image segmentation performance are conducted. The experimental results allow to recommend the proposed CNN for use in practice, as well as to determine effective conditions for the application of the proposed CNN.

Prospects for further research are to study the performance of the proposed CNN then abrupt changes in color and illumination, blurring, as well as the complex background areas are present on dermatological images, for example, containing clothes or fragments of the interior. In addition, it is advisable to use the proposed CNN in other problems of color image processing to segment statistical or spectral-statistical texture regions on a uniform or textured background.

ACKNOWLEDGEMENTS

The author express their deep gratitude to V. N. Krylov, Doctor of Technical Sciences, Professor of the Department of Applied Mathematics and Information Technologies, National University “Odessa Polytechnic” for valuable and constructive advice and comments while working on this paper.

REFERENCES

1. Kotvitska A. A., Carlo V. V. Research on the indicators of the prevalence of psoriasis in the world and Ukraine, *Zaporozhye Medical Journal,* 2013, № 3(78), pp. 38–42.
2. Jarad T. S., Dawood A. J. A quantitative technique for systematic monitoring of the treatment efficiency psoriasis lesion, *London Journal of Research in Computer Science and Technology*, 2019, Vol. 19, № 1, pp. 37–46.
3. Velasco J., Pascion C., Alberio J. W. et al. A smartphone-based skin disease classification using MobileNet CNN, *International Journal of Advanced Trends in Computer Science and Engineering,* 2019, Vol. 8, № 5, pp. 2632–2637. DOI: 10.30534/ijatcse/2019/116852019
4. Pal A., Chaturvedi A., Garain U. et. al. Severity grading of psoriatic plaques using deep CNN based multi-task learning, *Pattern Recognition: 23rd International Conference, ICPR, Cancun, Mexico, 4–8 December, 2016 : proceedings.* Piscataway, NJ, IEEE, 2016, pp. 1478–1483. DOI: 10.1109/ICPR.2016.7899846
5. Pal A., Garain U., Chandra A., Chatterjee R., Senapati S. Psoriasis skin biopsy image segmentation using deep convolutional neural network, *Computer Methods and Programs in Biomedicine*, 2018, Vol. 59, № 6 (1), pp. 59–69. DOI:10.1016/j.cmpb.2018.01.027
6. Jarad T. S., Dawood A. J. Accurate segmentation of psoriasis diseases images using k-means algorithm based on CIELAB (L*A*B) color space, *Journal of Theoretical and Applied Information Technology,* 2017, Vol. 95, № 17, pp. 4201–4210.
7. Pal A., Roy A., Sen K. et al. Mixture model based color clustering for psoriatic plaque segmentation, *Pattern Recognition : Third IAPR Asian Conference, ACPR, Kuala Lumpur, Malaysia, 3–6 November 2015 : proceedings.* Red Hook, NY, IEEE, 2015, pp. 376–380. DOI:10.1109/ACPR.2015.7486529
8. Volkova N. P. Detector quasi-periodic texture segmentation method for dermatologica images processing, *Herald of Advanced Information Technology*, 2019, Vol. 2, № 4, pp. 259–267. DOI: 10.15276/hait.04.2019.2.
9. Dash M., Londhe N. D., Ghosh S., Semwal A., Sonawane R. S. PsLSNet: automated psoriasis skin lesion segmentation using modified U-Net-based fully convolutional network, *Biomedical Signal Processing and Control,* 2019, Vol. 52, pp. 226–237. DOI: 10.1016/j.bspc.2019.04.002
10. Lin G.-S., Lai K.-T., Syu J.-M. et al. Instance segmentation based on deep convolutional neural networks and transfer learning for unconstrained psoriasis skin images, *Applied Scienses,* 2021, Vol. 11, 3155. DOI: 10.3390/app11073155
11. Subbotin S. A. The fractal dimension based quality metrics of data samples and dependence models, *Radio Electronics, Computer Science, Control*, 2017, № 2, pp. 70–81. DOI: 10.15588/1607-3274-2017-2-8
12. Leoshchenko S. D., Oliynyk A. O., Subbotin S. O., Hoffman E. O., Kornienko O. V. Method of structural adjustment of neural network models to ensure interpretability, *Radio electronics, computer science, management*, 2021, № 3, pp. 86–96.
13. Roslan R., Razly I. N. M., Sabri N., Ibrahim Z. Evaluation of psoriasis skin disease classification using convolutional neural network, *International Journal of Artificial Intelligence*, 2020, Vol. 9, № 2, pp. 349–355. DOI: 10.11591/ijai.v9.i2
14. Raza M. A., Liaqat M. S., Shoaib M. A fuzzy expert system design for diagnosis of skin diseases, *Advancements in Computational Sciences: Second International Conference, ICACS, Lahore, Pakistan, 18–20 February, 2019 : proceedings*, IEEE, 2019. pp. 1–7. DOI: 10.23919/ICACS.2019.8689140
15. George Y. M., Aldeen M., Garnavi R. Automatic scale severity assessment method in psoriasis skin images using local descriptors, *Journal of Biomedical and Health Informatics*, 2020, Vol. 24, № 2, pp. 577–585. DOI: 10.1109/JBHI.2019.2910883.
16. Mullangi P., Yarravarapu S. R., Kotipalli P., Urooj S. (ed.). Texture and clustering-based skin disease classification, Sensors and Image Processing. Singapore, Springer, 2018, pp. 103–110. DOI: 10.1007/978-981-10-6614-6_11
17. Munia T. T., Haque I. R., Aymond A. et. al. Automatic clustering-based segmentation and plaque localization in psoriasis digital images, Healthcare Innovations and Point-of-Care Technologies, *Special Topics Conference, IEEE-*

DOI 10.15588/1607-3274-2023-1-5

NIH, Bethesda Campus, MD, USA, 6–8 November, 2017 : proceedings, IEEE, 2017, pp. 113–116. DOI: 10.1109/HIC.2017.8227597
18. Roy K., Chaudhuri S. S., Ghosh S. et al. Skin disease detection based on different segmentation techniques, *Opto-Electronics and Applied Optics: International Conference, Optronix, Kolkata.* India, 18–20 March, 2019, proceedings, IEEE, 2019, pp. 70–74. DOI: 10.1109/OPTRONIX.2019.8862403
19. Liu X., Krylov V., Jun S. et al. Segmentation and identification of spectral and statistical textures for computer medical diagnostics in dermatology, *Mathematical Biosciences and Engineering,* 2022, Vol. 19, № 7, pp. 6923–6939. DOI: 10.1109/JBHI.2019.2910883.
20. Krylov V. N., Volkova N. P. Vector-difference texture segmentation method in technical and medical express diagnostic systems, *Herald of Advanced Information Technology*, 2020, Vol. 3, № 4, pp. 226–239. DOI: 10.15276/hait.04.2020.2
21. George Y. M., Aldeen M., Garnavi R. Automatic psoriasis lesion segmentation in two-dimensional skin images using multiscale superpixel clustering, *Journal of Medical Imaging*, 2017, Vol. 4, № 4, pp. 59–69. DOI: 10.1117/1.JMI.4.4.044004
22. Psoriasis: Symptoms, Treatment, Images and More – DermNet [Electronic resource]. Access mode: http:// dermnetnz.org/
23. Polyakova M., Ishchenko A., Volkova N., Pavlov O. The combining segmentation method of the scanned documents images with sequential division of the photo, graphics, and the text areas, *Eastern- European Journal of Enterprise Technologies,* 2018, Vol. 5, № 2, pp. 6–16. DOI: 10.15587/1729-4061.2018.142735
24. Polyakova M. V., Nesteryuk A. G. Improvement of the color text image binarization method using the minimum-distance classifier, *Applied Aspects of Information Technology*, 2021. Vol. 4, № 1, pp. 57–70. DOI: 10.15276/aait.01.2021.5
25. Akinlar C., Topal C. ColorED: color edge and segment detection by edge drawing, *Journal of Visual Communication and Image Representation*, 2017, Vol. 44, pp. 82–94. DOI: 10.1016/j.jvcir.2017.01.024
26. Gonzalez R. C., Woods R. E. Digital Image Processing (4rd Edition). NY, Pearson, 2017, 1192 p.
27. Ronneberger O., Fischer P., Brox T. U-Net: convolutional networks for biomedical image segmentation, *Medical Image Computing and Computer-Assisted Intervention*, 2015, Vol. 9351, pp. 234–241. DOI: 10.48550/arXiv.1505.04597

Received 07.11.2022.
Accepted 21.12.2022.

УДК 004.93

СЕГМЕНТАЦІЯ ЗОБРАЖЕНЬ ЗГОРТКОВОЮ НЕЙРОННОЮ МЕРЕЖЕЮ БЕЗ ПУЛІНГОВИХ ШАРІВ В СИСТЕМАХ ДІАГНОСТИКИ ДЕРМАТОЛОГІЧНИХ ЗАХВОРЮВАНЬ

Полякова М. В. – д-р техн. наук, доцент, професор кафедри прикладної математики та інформаційних технологій Національного університету «Одеська політехніка», Одеса, Україна.

АНОТАЦІЯ

Актуальність. Розглянуто задачу автоматизації процесу сегментації спектрально-статистичних текстурних зображень. Об’єктом дослідження є обробка зображень у системах діагностики дерматологічних захворювань. Метою дослідження є покращення якості сегментації кольорових псоріазних зображень шляхом розробки згорткової нейронної мережі глибокого навчання без пулінгових шарів.

Метод. Запропоновано згорткову нейронну мережу для обробки трьохканального псоріазного зображення заданого розміру. Початкові кольорові зображення було масштабовано до заданого розміру, а потім подано на вхідний шар нейронної мережі. Архітектура запропонованої нейронної мережі складається з чотирьох згорткових шарів з пакетною нормалізацією та функцією активації ReLU. Карти ознак із виходу цих шарів передавалися до згорткового шару 1×1 з функцією активації Softmax. Отримані карти ознак подавалися до шару класифікації пікселів зображення. При сегментуванні зображень згорткові та пулінгові шари оцінюють ознаки фрагментів зображення, а повністю зв’язані шари класифікують отримані вектори ознак, виконуючи розбиття зображення на однорідні сегменти. Ознаки сегментації оцінювалися в результаті навчання мережі а допомогою зображень, сегментованих експертом. Отримані ознаки стійкі до завад та спотворень зображень. Об’єднання результатів сегментації в різних масштабах визначається архітектурою мережі. Пулінгові шари включалися в архітектуру запропонованої згорткової нейронної мережі, оскільки вони зменшують розмір карт ознак порівняно з розміром початкового зображення та можуть знизити якість сегментації невеликих псоріазних плям та псоріазних плям складної форми.

Результати. Запропоновану згорткову нейронну мережу реалізовано програмно і досліджено при вирішенні задачі сегментації псоріазних зображень.

Висновки. Використання запропонованої згорткової нейронної мережі дозволило підвищити якість сегментації зображень бляшкового та крапельного псоріазу, особливо на границях плям. Перспективи подальших досліджень можуть полягати у дослідженні якості сегментації зображень запропонованою згортковою нейронною мережею, якщо на дерматологічних зображеннях присутні різкі зміни кольору та освітленості, розмиття, а також фрагменти складного фону, наприклад, що містять одяг або фрагменти інтер’єру. Доцільно. використовувати запропоновану згорткову нейронну мережу в інших задачах обробки кольорових зображень для сегментації статистичних або спектрально-статистичних текстурних областей на однорідному або текстурованому фоні.

КЛЮЧОВІ СЛОВА: псоріазне зображення, сегментація зображення, згорткова нейронна мережа, пулінговий шар, кольоровий простір, глибоке навчання.

DOI 10.15588/1607-3274-2023-1-5

ЛІТЕРАТУРА

1. Kotvitska A. A. Research on the indicators of the prevalence of psoriasis in the world and Ukraine / A. A. Kotvitska, V. V. Carlo // Zaporozhye Medical Journal. – 2013. – № 3(78). – P. 38–42.
2. Jarad T. S. A quantitative technique for systematic monitoring of the treatment efficiency psoriasis lesion / T. S. Jarad, A. J. Dawood // London Journal of Research in Computer Science and Technology. – 2019. – Vol. 19, № 1. – P. 37–46.
3. A smartphone-based skin disease classification using MobileNet CNN / [J. Velasco, C. Pascion, J. W. Alberio et al.] // International Journal of Advanced Trends in Computer Science and Engineering. – 2019. – Vol. 8, № 5. – P. 2632–2637. DOI: 10.30534/ijatcse/2019/116852019
4. Severity grading of psoriatic plaques using deep CNN based multi-task learning / [A. Pal, A. Chaturvedi, U. Garain et al.] // Pattern Recognition: 23rd International Conference, ICPR, Cancun, Mexico, 4–8 December, 2016 : proceedings. – Piscataway, NJ, IEEE: 2016. – P. 1478–1483. DOI: 10.1109/ICPR.2016.7899846
5. Psoriasis skin biopsy image segmentation using deep convolutional neural network / [A. Pal, U. Garain, A. Chandra et al.] // Computer Methods and Programs in Biomedicine. – 2018. – Vol. 59, № 6 (1). – P. 59–69. DOI:10.1016/j.cmpb.2018.01.027
6. Jarad T. S., Dawood A. J. Accurate segmentation of psoriasis diseases images using k-means algorithm based on CIELAB (L*A*B) color space / T. S. Jarad, A. J. Dawood // Journal of Theoretical and Applied Information Technology. – 2017. – Vol. 95, № 17. – P. 4201–4210.
7. Mixture model based color clustering for psoriatic plaque segmentation / [A. Pal, A. Roy, K. Sen et al.] // Pattern Recognition : Third IAPR Asian Conference, ACPR, Kuala Lumpur, Malaysia, 3–6 November 2015 : proceedings. – Red Hook, NY, IEEE: 2015. – P. 376–380. DOI:10.1109/ACPR.2015.7486529
8. Volkova N. P. Detector quasi-periodic texture segmentation method for dermatologica images processing / N. P. Volkova // Herald of Advanced Information Technology. – 2019. – Vol. 2, № 4. – P. 259–267. DOI: 10.15276/hait.04.2019.2.
9. PsLSNet: automated psoriasis skin lesion segmentation using modified U-Net-based fully convolutional network / [M. Dash, N. D. Londhe, S. Ghosh et al.] // Biomedical Signal Processing and Control. – 2019. – Vol. 52. – P. 226–237. DOI: 10.1016/j.bspc.2019.04.002
10. Instance segmentation based on deep convolutional neural networks and transfer learning for unconstrained psoriasis skin images / [G.-S. Lin, K.-T. Lai, J.-M. Syu et al.] // Applied Scienses. – 2021. – Vol. 11, 3155. DOI: 10.3390/app11073155
11. Subbotin S. A. The fractal dimension based quality metrics of data samples and dependence models / S. A. Subbotin // Radio Electronics, Computer Science, Control. – 2017. – № 2. – P. 70–81. DOI: 10.15588/1607-3274-2017-2-8
12. Метод структурного доналаштування нейромережевих моделей для забезпечення інтерпретабельності / [С. Д. Леощенко, А. О. Олійник, С. О. Субботін и др.] // Радіоелектроніка, інформатика, управління. – 2021. – № 3. – С. 86–96.
13. Evaluation of psoriasis skin disease classification using convolutional neural network / [R. Roslan, I. N. M. Razly, N. Sabri, Z. Ibrahim] // International Journal of Artificial Intelligence. – 2020. – Vol. 9, № 2. – P. 349–355. DOI: 10.11591/ijai.v9.i2
14. Raza M. A. A fuzzy expert system design for diagnosis of skin diseases / M. A. Raza, M. S. Liaqat, M. Shoaib // Advancements in Computational Sciences: Second International Conference, ICACS, Lahore, Pakistan, 18–20 February, 2019 : proceedings. – IEEE: 2019. P. 1–7. DOI: 10.23919/ICACS.2019.8689140
15. George Y. M. Automatic scale severity assessment method in psoriasis skin images using local descriptors / Y. M. George, M. Aldeen, R. Garnavi // Journal of Biomedical and Health Informatics. – 2020. – Vol. 24, № 2. – P. 577–585. DOI: 10.1109/JBHI.2019.2910883.
16. Mullangi P. Texture and clustering-based skin disease classification / P. Mullangi, S. R. Yarravarapu, P. Kotipalli // Sensors and Image Processing / S. Urooj (ed.). – Singapore, Springer: 2018. – P. 103–110. DOI: 10.1007/978-981-10-6614-6_11
17. Automatic clustering-based segmentation and plaque localization in psoriasis digital images / [T. T. Munia, I. R. Haque, A. Aymond et. al.] // Healthcare Innovations and Point-of-Care Technologies: Special Topics Conference, IEEE-NIH, Bethesda Campus, MD, USA, 6–8 November, 2017 : proceedings. – IEEE: 2017. – P. 113–116. DOI: 10.1109/HIC.2017.8227597
18. Skin disease detection based on different segmentation techniques / [K. Roy, S. S. Chaudhuri, S. Ghosh et al.] // Opto-Electronics and Applied Optics: International Conference, Optronix, Kolkata, India, 18–20 March, 2019 : proceedings. – IEEE: 2019. P. 70–74. DOI: 10.1109/OPTRONIX.2019.8862403
19. Segmentation and identification of spectral and statistical textures for computer medical diagnostics in dermatology / [X. Liu, V. Krylov, S. Jun et al.] // Mathematical Biosciences and Engineering. – 2022. – Vol. 19, № 7. – P. 6923–6939. DOI: 10.1109/JBHI.2019.2910883.
20. Krylov V. N. Vector-difference texture segmentation method in technical and medical express diagnostic systems / V. N. Krylov, N. P. Volkova // Herald of Advanced Information Technology. – 2020. – Vol. 3, № 4. – P. 226–239. DOI: 10.15276/hait.04.2020.2
21. George Y. M. Automatic psoriasis lesion segmentation in two-dimensional skin images using multiscale superpixel clustering / Y. M. George, M. Aldeen, R. Garnavi // Journal of Medical Imaging. – 2017. – Vol. 4, № 4. – P. 59–69. DOI: 10.1117/1.JMI.4.4.044004
22. Psoriasis: Symptoms, Treatment, Images and More – DermNet [Electronic resource]. – Access mode: http:// dermnetnz.org/
23. The combining segmentation method of the scanned documents images with sequential division of the photo, graphics, and the text areas / [M. Polyakova, A. Ishchenko, N. Volkova, O. Pavlov] // Eastern- European Journal of Enterprise Technologies. – 2018. – Vol. 5, № 2. – P. 6–16. DOI: 10.15587/1729-4061.2018.142735
24. Polyakova M. V. Improvement of the color text image binarization method using the minimum-distance classifier / M. V. Polyakova, A. G. Nesteryuk // Applied Aspects of Information Technology. – 2021. – Vol. 4, № 1. – P. 57–70. DOI: 10.15276/aait.01.2021.5
25. Akinlar C. ColorED: color edge and segment detection by edge drawing / C. Akinlar, C. Topal // Journal of Visual Communication and Image Representation. – 2017. – Vol. 44. – P. 82–94. DOI: 10.1016/j.jvcir.2017.01.024
26. Gonzalez R. C., Woods R. E. Digital Image Processing (4rd Edition) / R. C. Gonzalez, R. E. Woods. – NY : Pearson, 2017. – 1192 p.
27. Ronneberger O. U-Net: convolutional networks for biomedical image segmentation / O. Ronneberger, P. Fischer, T. Brox // Medical Image Computing and Computer-Assisted Intervention. – 2015. – Vol. 9351. – P. 234–241. DOI: 10.48550/arXiv.1505.04597

DOI 10.15588/1607-3274-2023-1-5